I) Why and how to harvest energy from sun light

II) Excitonic solar cells

III) Halid Perovskites for solar cells

Best Research-Cell Efficiencies

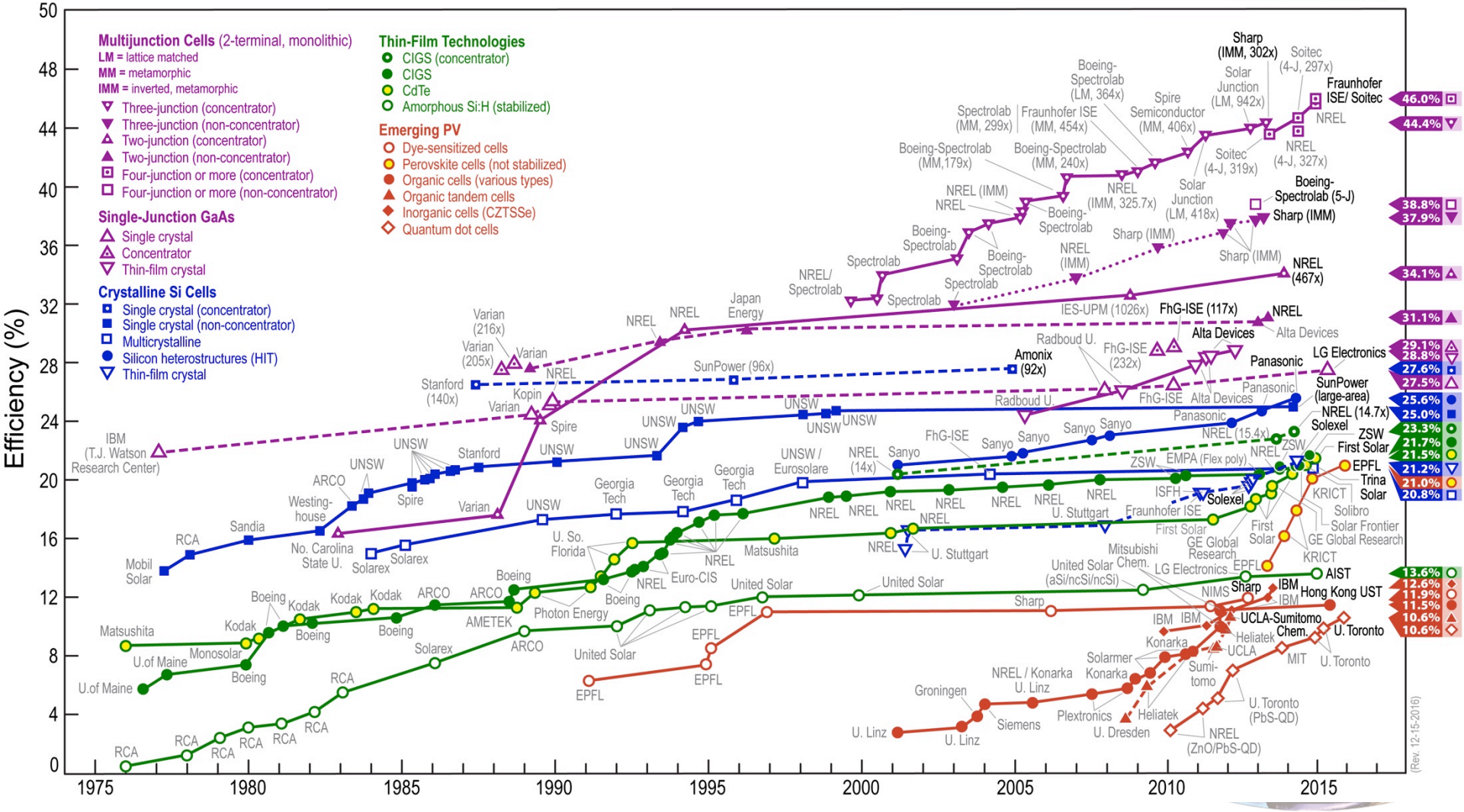

Halid perovskites

- Properties and devices
- Electronic structure
- Electronic transport and quantum effects

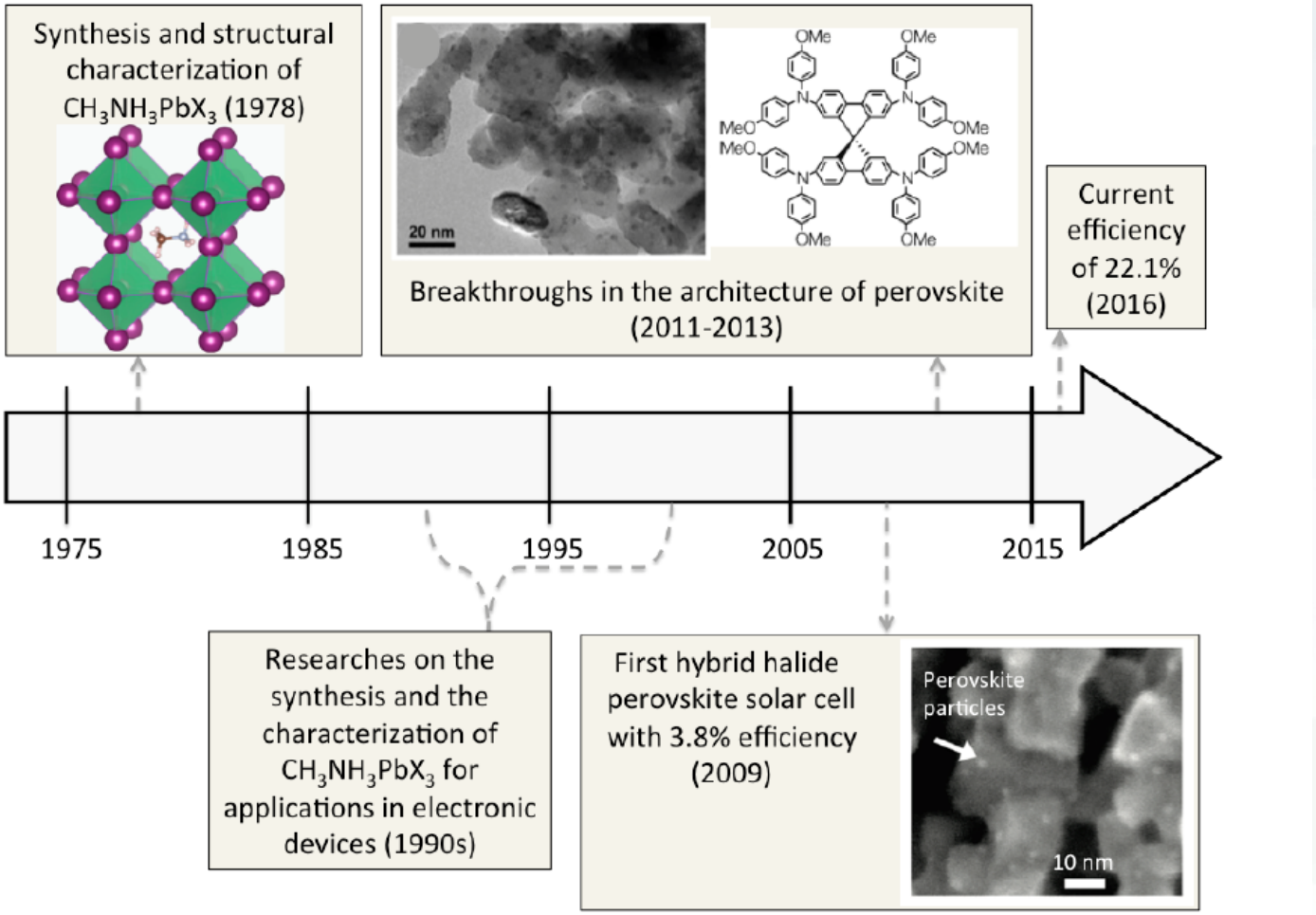

Figure 1.1: Timeline of research over structure, synthesis and optoelectronic properties of hybrid halide perovskite and important discoveries in the improvement of the perovskite solar cell efficiency.

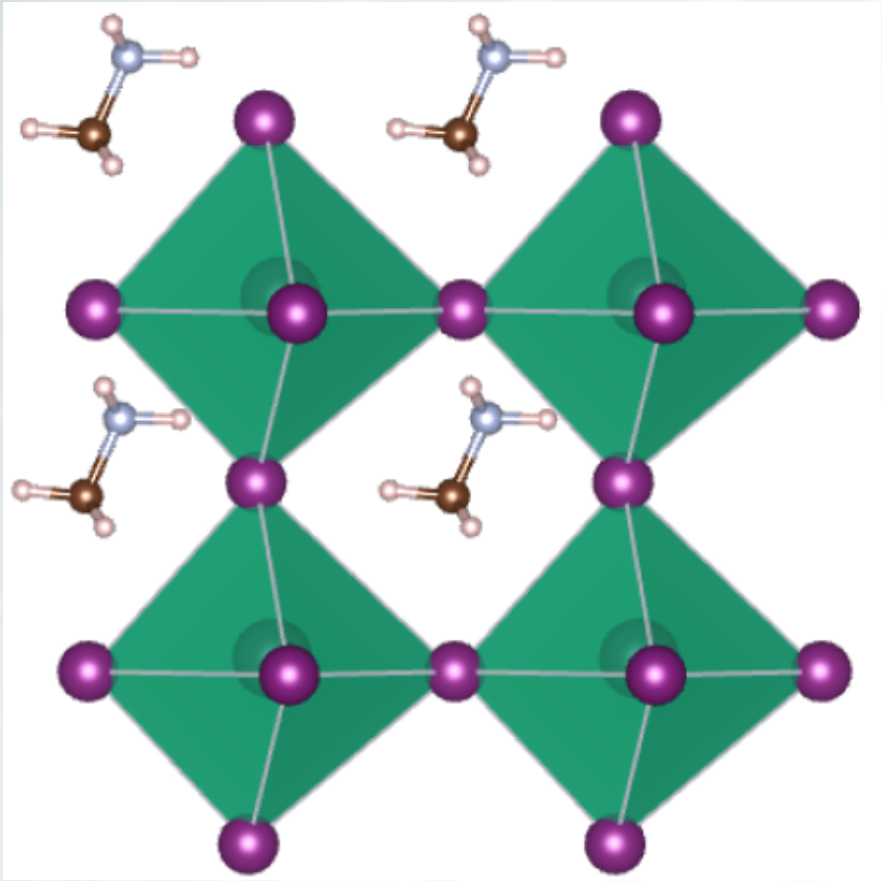

Figure 2.1: Polyhedral representation of the crystal structure of $CH_3NH_3PbI_3$. The atoms are respectively: Pb (in grey) located at the center of each octahedron, I (in purple) at the corners of each octahedron, C (in light blue), N (in brown) and H (in pink). For $CH_3NH_3^+$ cations, a ball-and-stick model is used.

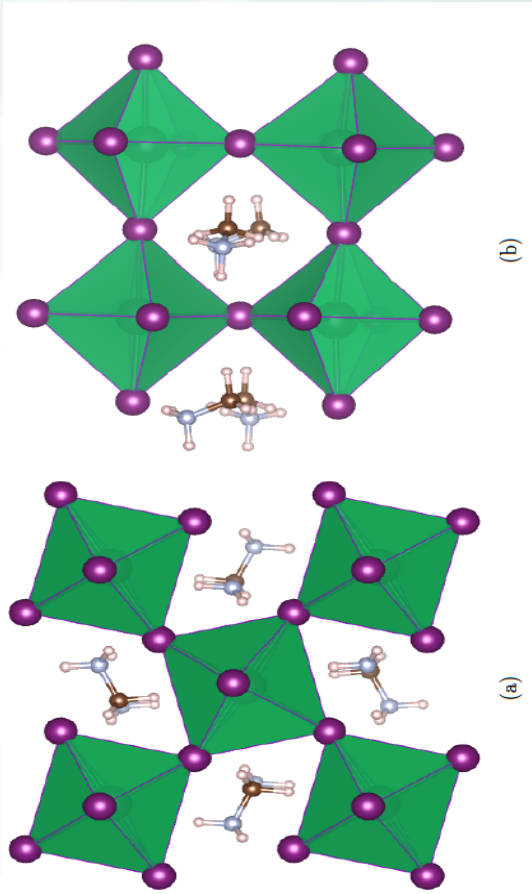

Figure 2.2: Polyhedral representation of the different polymorphs for the organic-inorganic halide perovskite $CH_3NH_3PbI_3$, depending on the temperature: (a) Orthorhombic ($Pnma$) structure stable for $T < 162.2\,K$, (b) Tetragonal structure ($I4/mcm$) stable for $162.2 \leq T < 327.4\,K$, (c) Cubic structure ($Pm\bar{3}m$) stable for $T \geq 327.4\,K$. Atoms are represented as spheres: Pb are in grey and located at the center of each octahedron, I are in purple at the corners of each octahedron, C are in light blue, N are in brown, and H are in pink. For methylammonium cations, a ball-and-stick model is used.

Synthesis and stability : advantages and weaknesses

- Easy process at low cost
- But low resistance to moisture
- Contains lead
- Hysteresis problems…

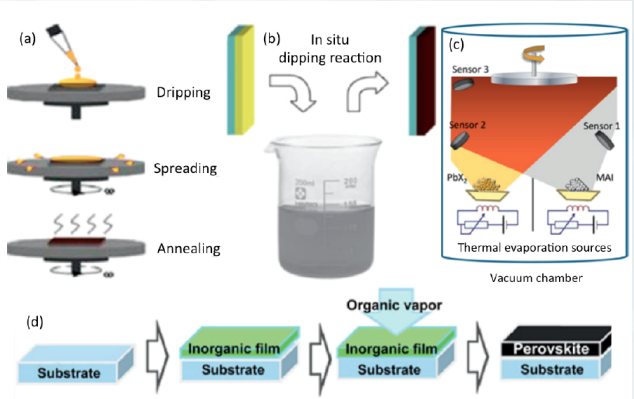

Figure 2.3: Main deposition methods to prepare perovskite active layers: (a) One-step precursor deposition, (b) two-step sequential deposition method, (c) dual-source vapor deposition, and (d) vapor-assisted solution process [3].

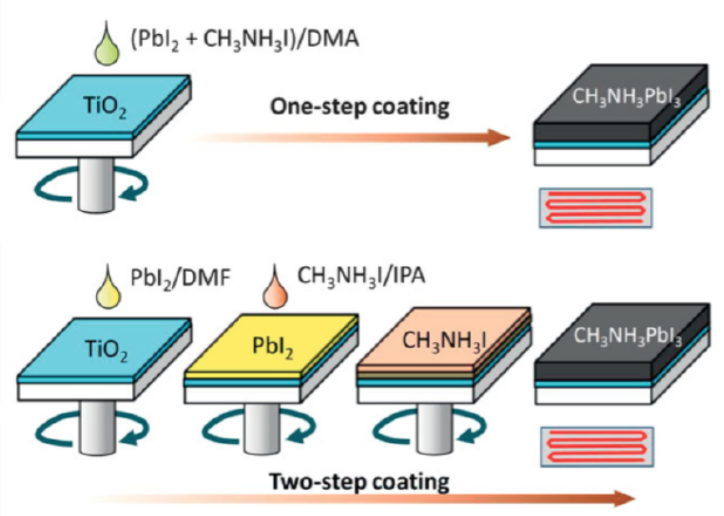

Figure 2.4: Schematic of one-step and two step coating methods to deposit $CH_3NH_3PbI_3$ perovskite thin films. For the one-step procedure, a single precursor solution containing the lead halide PbI_2 and the methylammonium halide CH_3NH_3I is used. For the two-step coating method, the methylammonium iodide solution reacts with the initially spin-coated PbI_2 film. DMA refers to dimethylacetamide, DMF to dimethylformamide and IPA to isopropyl alcohol. [4]

Great electronic characteristics : Absorbance, gap, mobility, lifetime

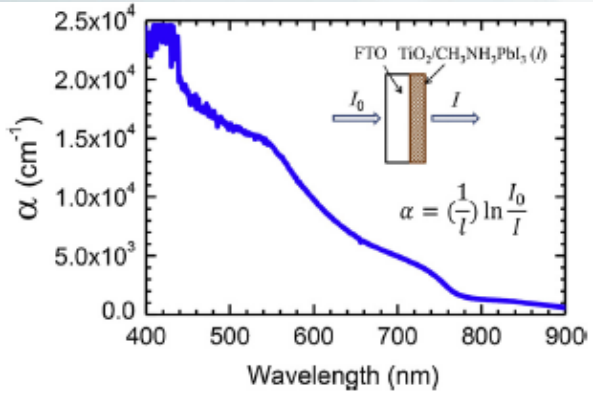

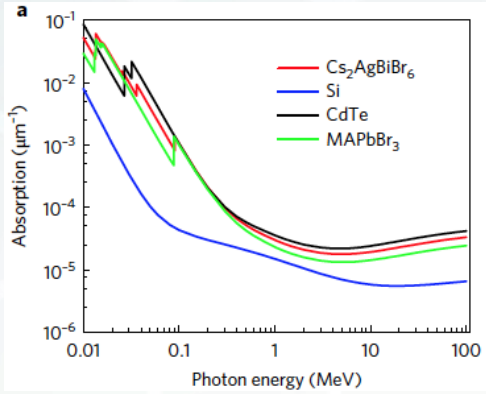

Table 1. Band Gaps (E_g) for Select MHPs with Variable Chemistries and Dimensionality[a]

compound	E_g (eV)	type	dimension
$CH_3NH_3PbI_3$	1.61	direct	3D
$CH_3NH_3Pb(I_{1-x}Br_x)_3$	1.57 ($x = 0$); 2.29 ($x = 1$)		
$CH_3NH_3PbCl_3$	2.88		
$CH_3NH_3(Pb_{1-x}Sn_x)I_3$[b]	1.55 ($x = 0$); 1.17 ($x = 0.5$); 1.30 ($x = 1$)		
$HC(NH_2)_2Pb(I_{1-x}Br_x)_3$	1.48 ($x = 0$); 2.21 ($x = 1$)		

Table 3. Measured Ranges for L_D and μ for Various Metal Halide Perovskites

compound	sample type	μ ($cm^2 V^{-1} s^{-1}$)	L_D (μm)	τ (ns)
$CH_3NH_3PbI_3$	thin film (solution)	1.4[b]	0.13[b]	4.5
		0.9[c]	0.09[c]	
		0.66[b]	0.13[b]	9.6
		0.43[c]	0.11[c]	
		8.2[b,c]	1.2	67
		12.5[b]	–	–
		7.5[c]		
		2[b]	2.3[b]	1000[a]
		1[c]	1.6[c]	
		11[b,c]	~ 1[b,c]	~40
		3.1[b,c]	1.27[b,c]	50
		35[b,c]	2.5[b,c]	~70
	PV device	–	~ 1[b,c]	–
		–	~ 1[b,c]	–
	pellet	66[b]	–	–
	single crystal	2.5[b,c]	2–8[b,c]	1032
		67[b,c]	9.7	570
		25[b]	175	90,000
		160[c]		
$CH_3NH_3Pb(I_{1-x}Cl_x)_3$	thin film (solution)	1.6[b]	1.07[b]	273
		2.1[c]	1.21[c]	
		11.6[b,c]	2.4[b,c]	200
	thin film (vapor)	33[b,c]	2.66[b,c]	83
	PV device	–	1.2[b]	–
			1.9[c]	
		–		–
		–	~ 1.4[b,c]	–
$CH_3NH_3Pb(Br_{1-x}Cl_x)_3$	PV device		0.15–0.45[b]	–
$CH_3NH_3PbBr_3$	thin film (vapor assisted)	8.9[b]	1.06[b]	51
		9.4[c]	1.08[c]	
	single crystal	20–115[b,c]	3–17[b,c]	357–978
		24	4.2	300
$CH_3NH_3PbCl_3$	single crystal	42[b,c]	3–8.5[b,c]	83–662
$CH(NH_2)_2PbI_3$	thin film	0.16[b]	0.18[b]	~75
		3.5[c]	0.82[c]	
	thin film	27[b,c]	3.1	~140
$CH(NH_2)_2PbBr_3$		14[b,c]	1.3	~50

Low excitonic energy and unstable excitons at room temperature

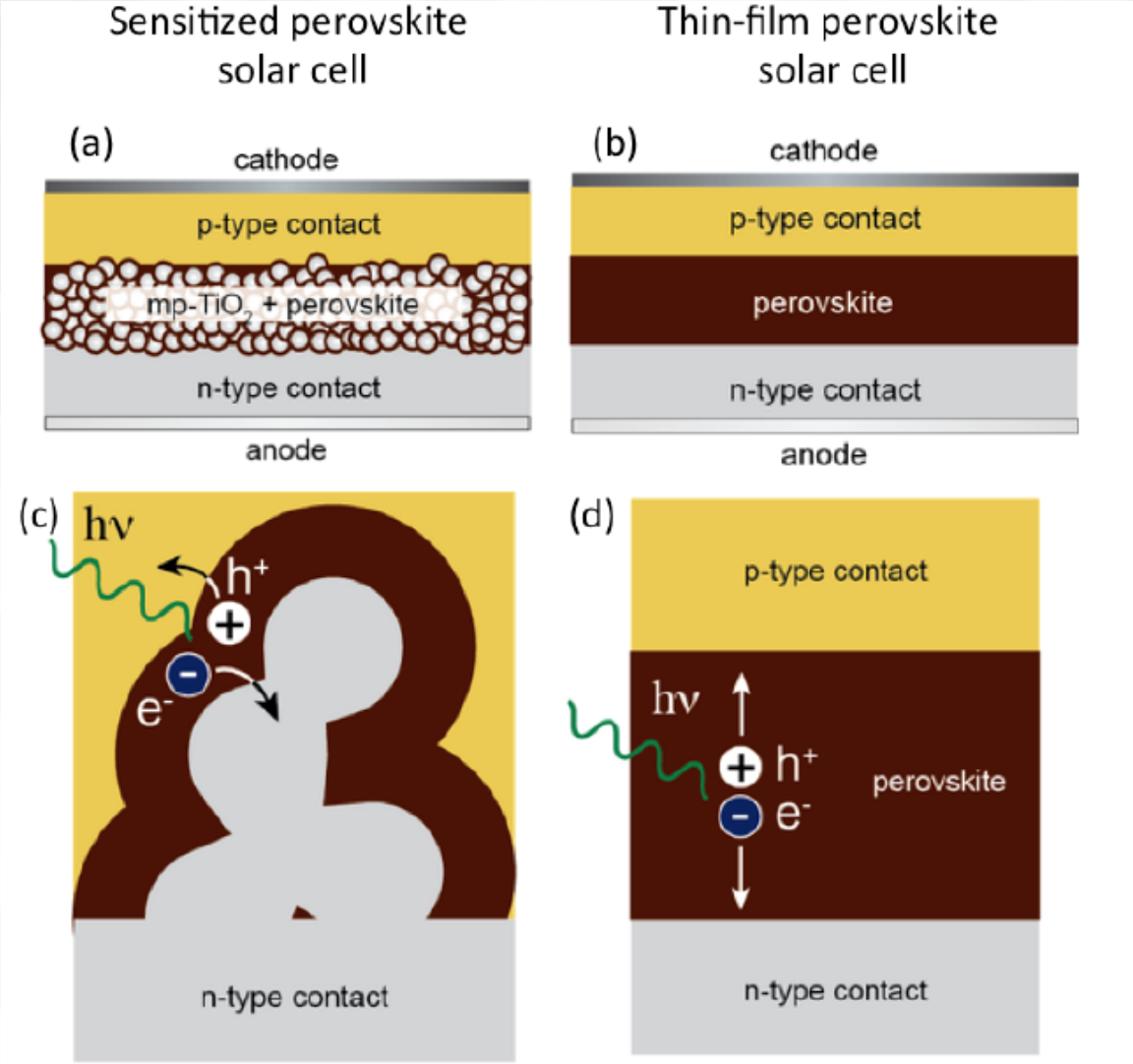
Sensitized perovskite solar cell
Thin-film perovskite solar cell
(a)
cathode
p-type contact
mp-TiO2 + perovskite
n-type contact
anode
(b)
cathode
p-type contact
perovskite
n-type contact
anode
(c)
hν
h+
e-
n-type contact
(d)
p-type contact
hν
h+
e-
perovskite
n-type contact

Direct X ray detection

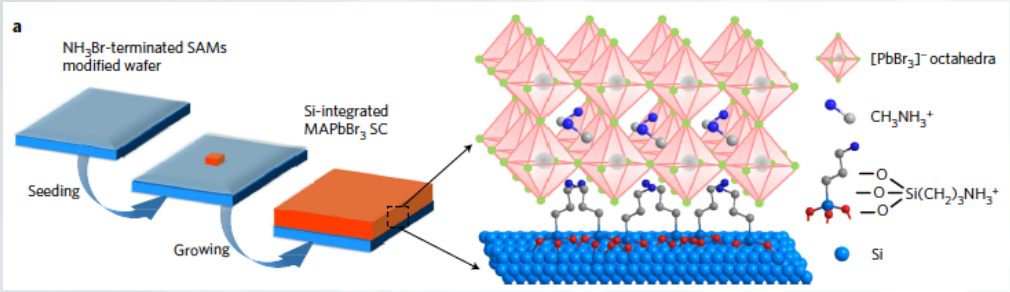

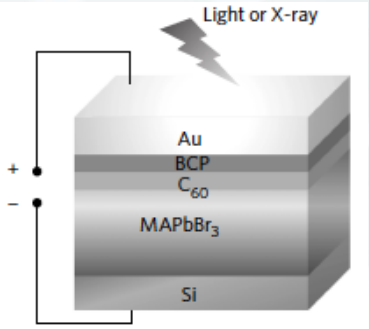

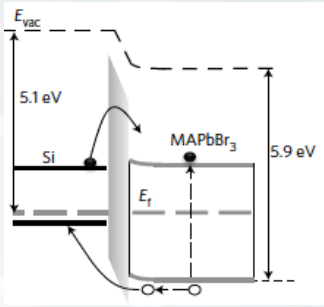

Wei Wei[1†], Yang Zhang[1†], Qiang Xu[2], Haotong Wei[1], Yanjun Fang[1], Qi Wang[1], Yehao Deng[1], Tao Li[3], Alexei Gruverman[3], Lei Cao[2] and Jinsong Huang[1*]

NATURE PHOTONICS | VOL 11 | MAY 2017 |

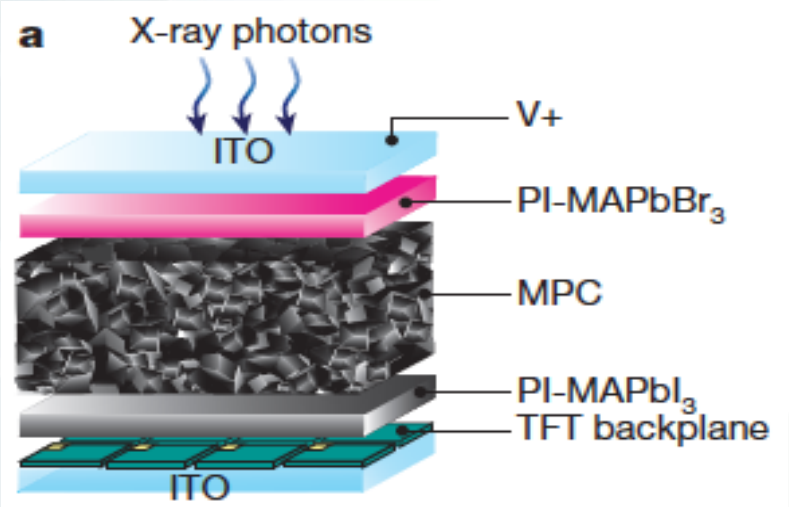

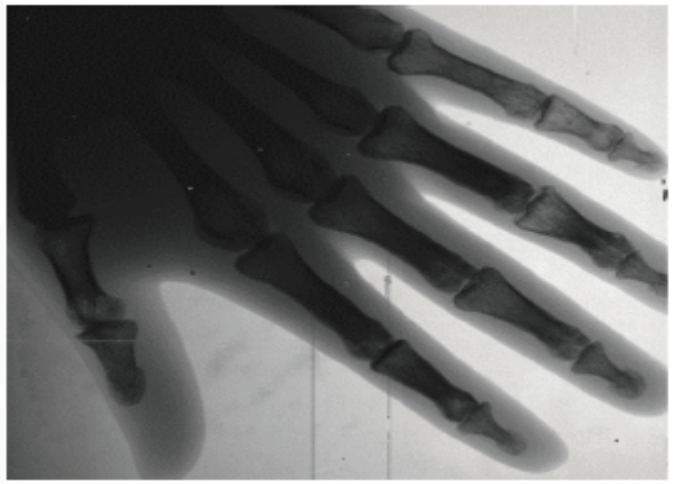

Printable organometallic perovskite enables large-area, low-dose X-ray imaging

Yong Churl Kim[1], Kwang Hee Kim[1], Dae-Yong Son[2], Dong-Nyuk Jeong[2], Ja-Young Seo[2], Yeong Suk Choi[1], In Taek Han[1], Sang Yoon Lee[1] & Nam-Gyu Park[2]

5 OCTOBER 2017 | VOL 550 | NATURE | 87

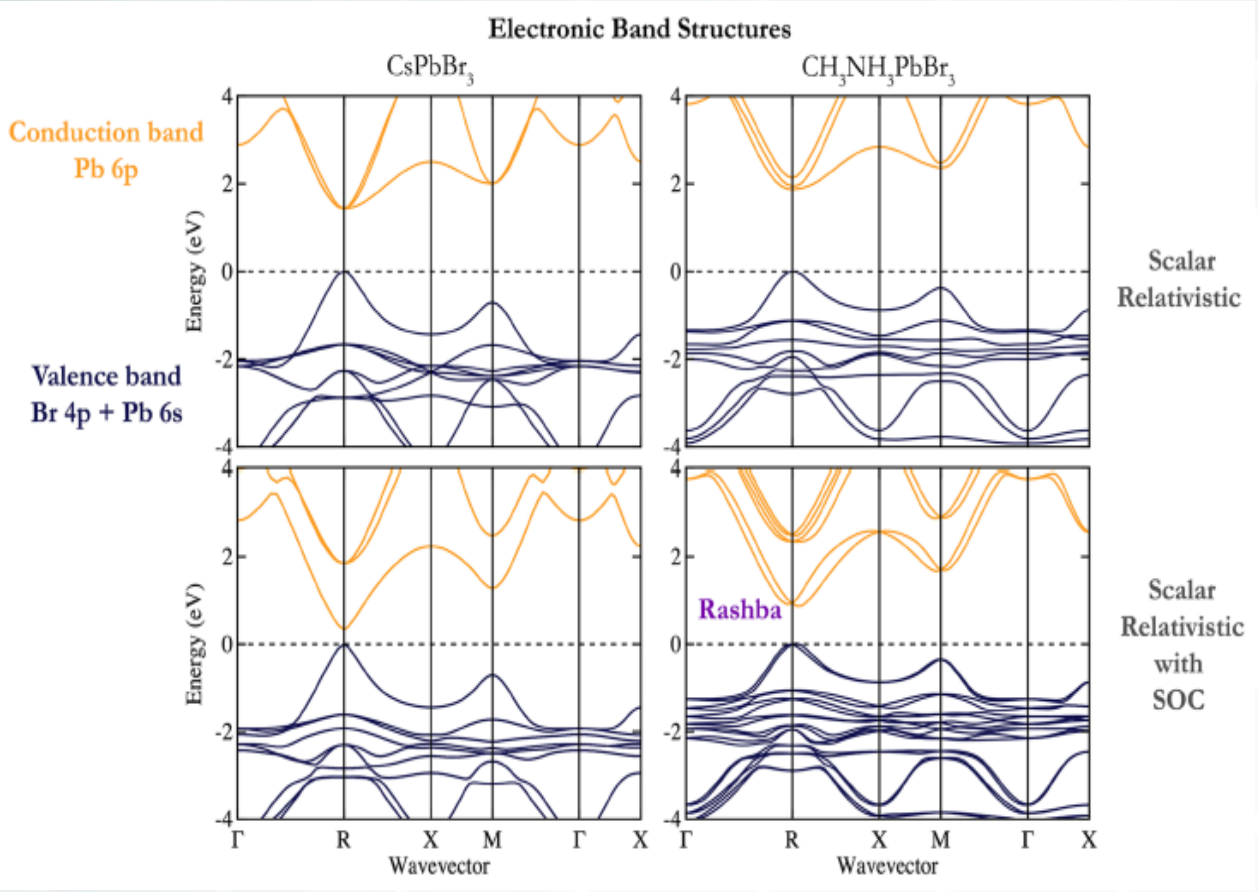

FIG. 3. The electronic band structures of the inorganic perovskite $CsPbBr_3$ and hybrid perovskite $CH_3NH_3PbBr_3$ in the cubic phase. An effect of the organic cation is to widen the bandgap located at the R point due to the larger lattice constant. Spin-orbit coupling reduces the bandgap in both materials. The presence of $CH_3NH_3^+$ in the hybrid perovskite results in a noncentrosymmetric crystal, with an associated relativistic Rashba-Dresselhaus splitting of the lower conduction band. While the labels of the special points are those of the cubic perovskite structure (space group $Pm\bar{3}m$), the static model of the hybrid perovskite formally has $P1$ symmetry. Points equivalent for a cubic crystal (e.g., $M = \frac{1}{2}, \frac{1}{2}, 0$; $M' = 0, \frac{1}{2}, \frac{1}{2}$; $M'' = \frac{1}{2}, 0, \frac{1}{2}$) are inequivalent here.

ARPES measurements on $MAPbI_3$

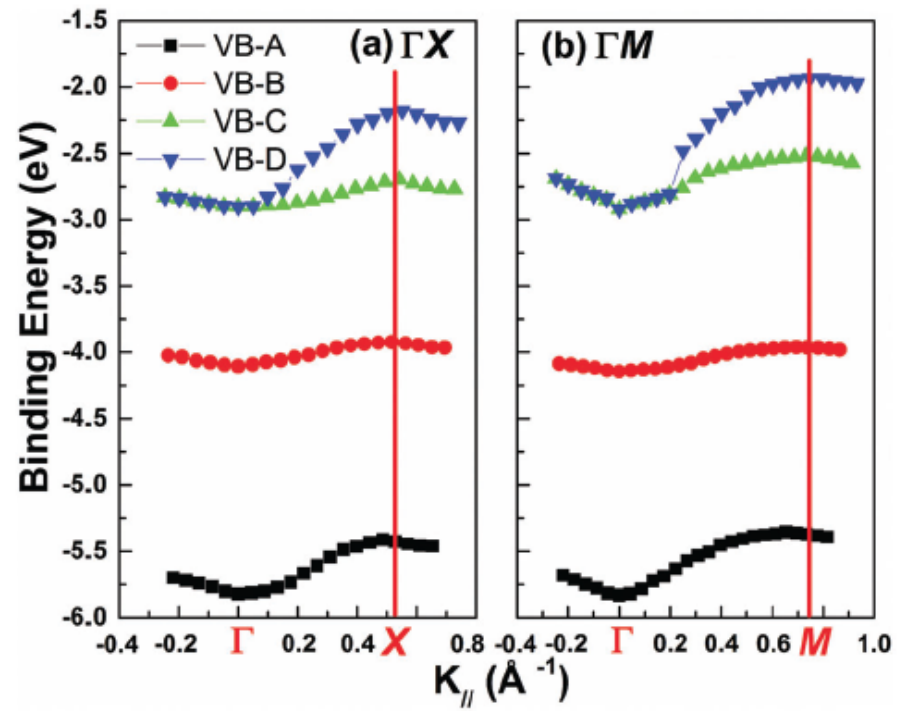

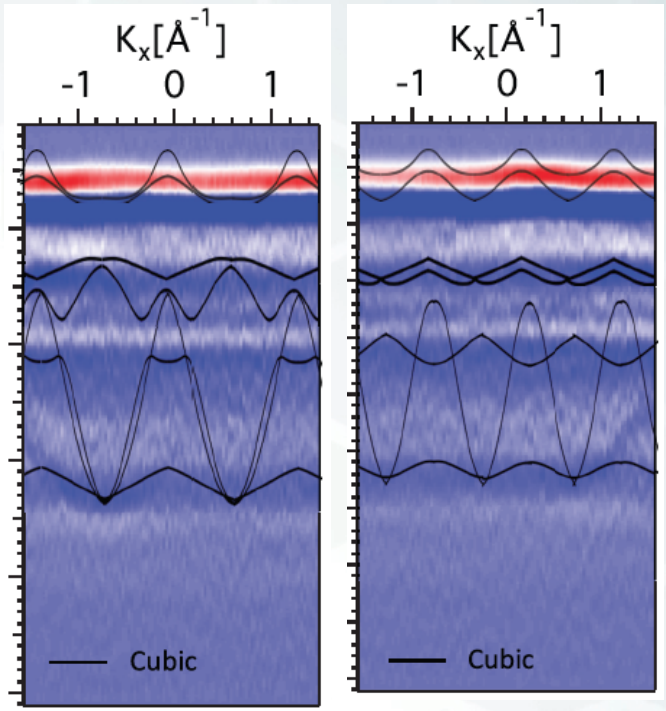

MΓM *MXM*

effective hole mass of $\sim 0.59 m_0$

spectral width
250 meV FWHM

Cite this: *Phys. Chem. Chem. Phys.*, 2017, **19**, 5361

J. Phys. D: Appl. Phys. **50** (2017) 26LT02

Tight-binding model

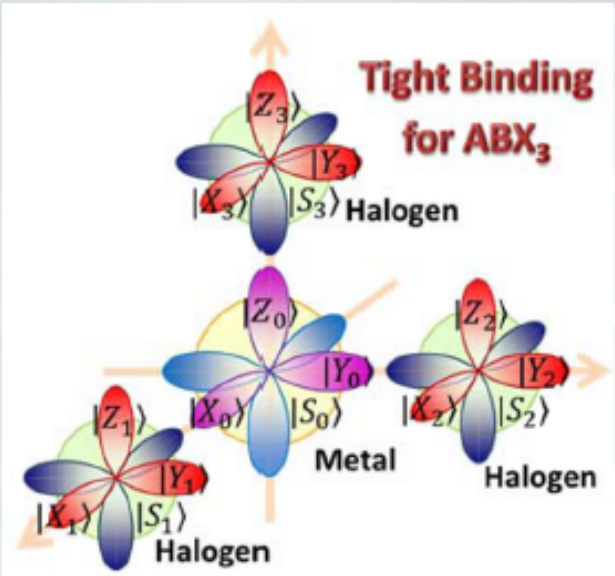

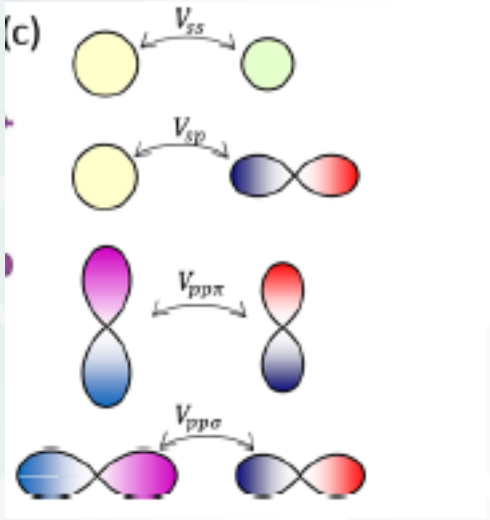

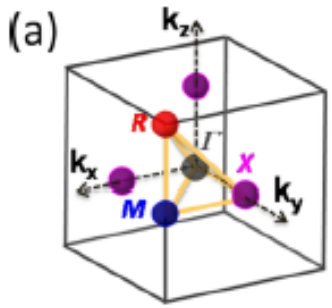

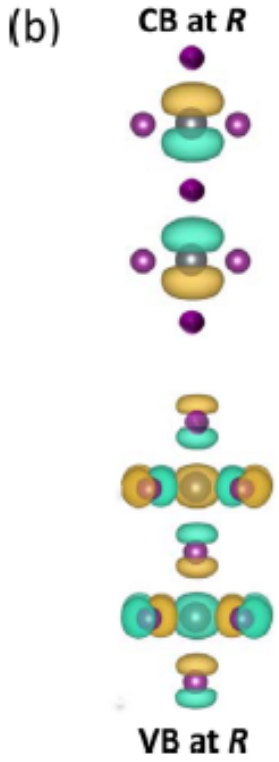

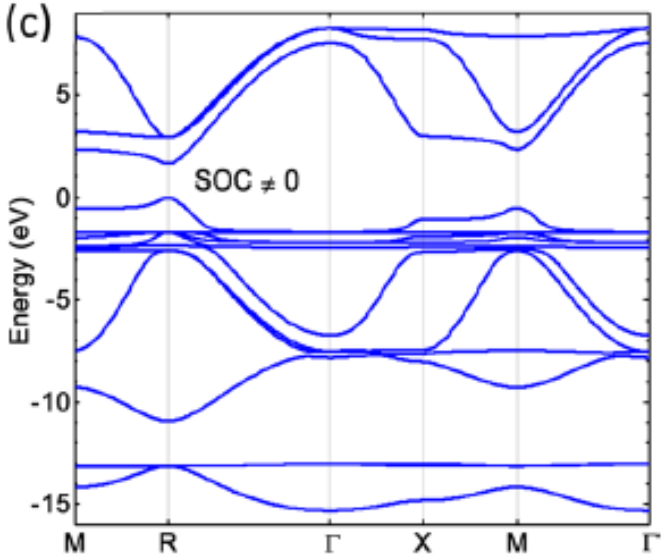

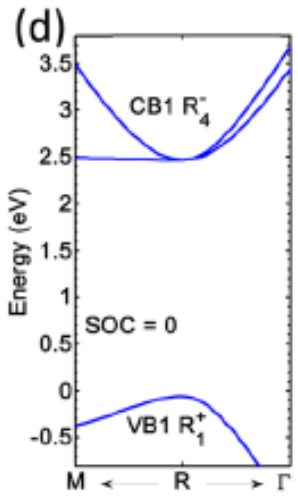

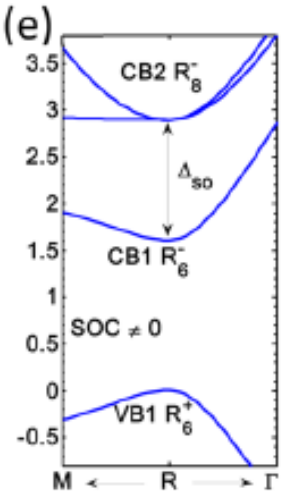

Charge transport, Mobility, mass, scattering time, mean-free path

- $\mu = e\tau/m$
- Mobility μ : 5-50 cm2/Vs
- Band effective mass m : 0.1-0.5 me
- Scattering time $\tau = \mu$ m/e is short of a few Femto seconds
- Mean-free path (room temperature) l=0.5 nm [m/0.2me]$^{1/2}$ ($\mu/100$ cm2/Vs)

- Very short mean-free path comparable to the unit cell size

- Polaron hypothesis : m= 4-12 me. Larger mean-free path but still smaller than the polaron size (Rp= 2-3 nm)

- **Semi-classical theory of transport seems not valid !**

Electronic structure modelisation

- Tight binding with first neighbor interaction only
- S and P orbitals of both iodine and lead are considered
- Orbital couplings computed *ab initio* *(Boyer-Richard et al. 2016)*
- The dipolar moment of the Ma molecule can generate disorder on the onsite energy of Pb and I
- The coupling between orbitals can also be disturbed due to disorder on atomic position
- Experimental basis for the intensity of the disorder (Lee *et al*. 2017)

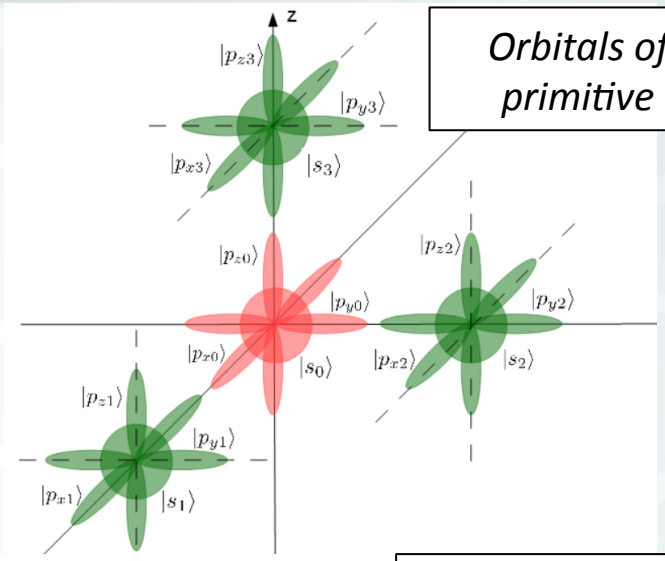

Orbitals of the primitive cell

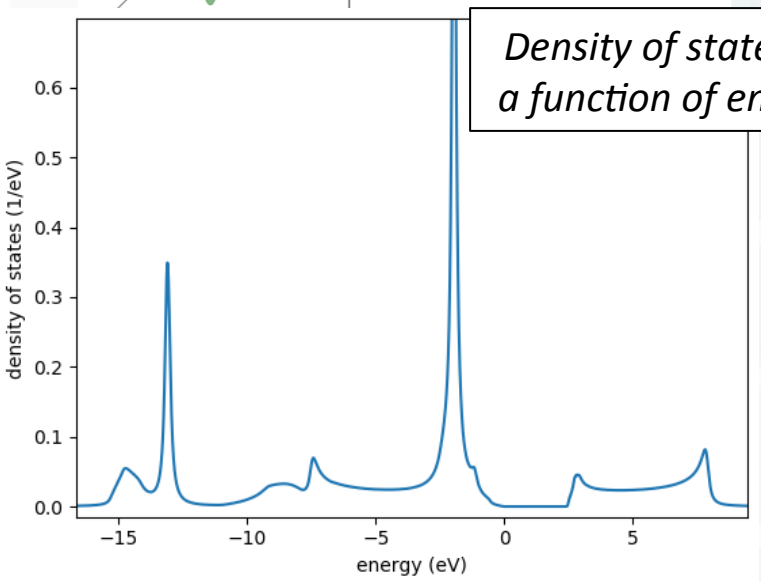

Density of states as a function of energy

Impact of different types of disorder

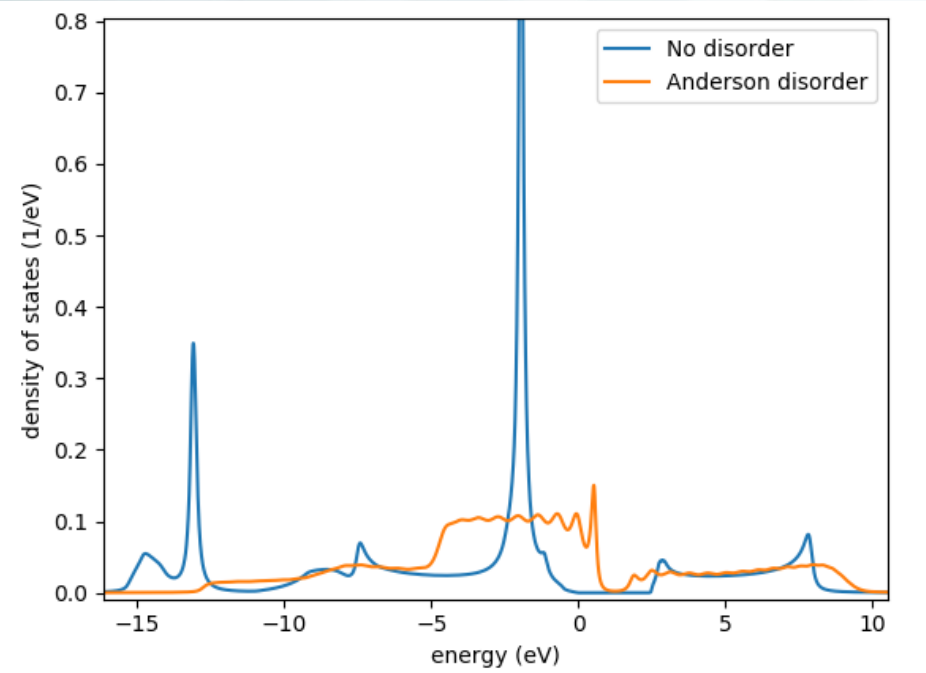

Density of states as a function of energy for the ordered system (blue) and with Anderson's disorder (orange)

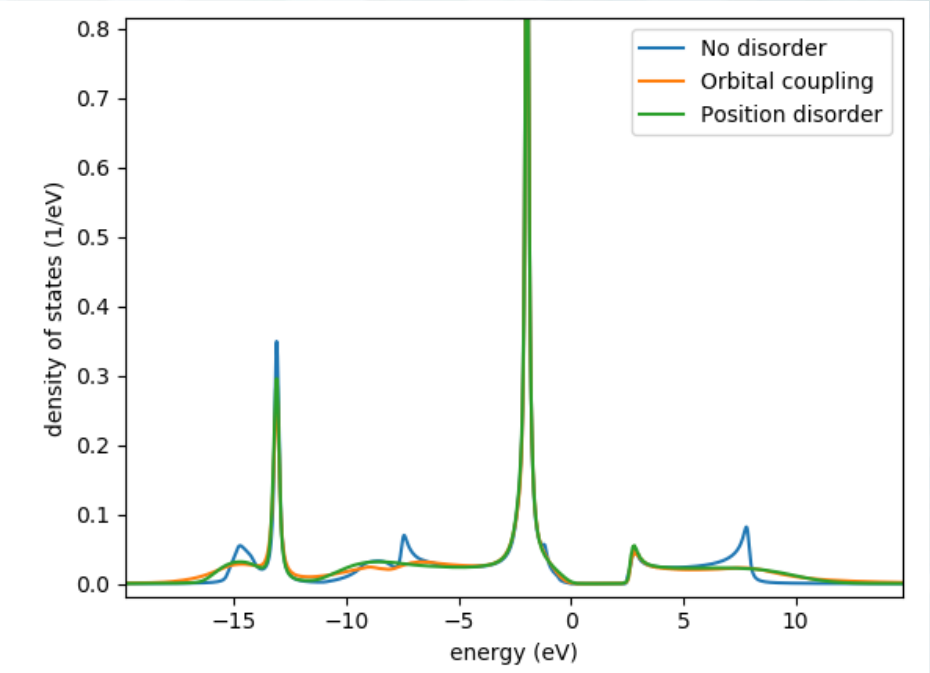

Density of states as a function of energy for the ordered system (blue), Orbital coupling disorder(orange), and position disorder (green)

Anderson's disorder is discarded as it fills the semiconductor gap of the material. Both disorders on orbital couplings and position maintain the value and position of the gap and will therefore be studied.

Electronic transport and diffusion

- Temporal propagation of the wave function solved numerically
- Computation of the mean squared displacement : ΔX^2
- Electronic diffusivity :

$$D = \frac{\Delta X^2}{t}$$

- Electronic mobility observed experimentally : 5~50 cm²/V.s

$$\mu = \frac{eD}{2k_bT}$$

- Three different types of diffusion

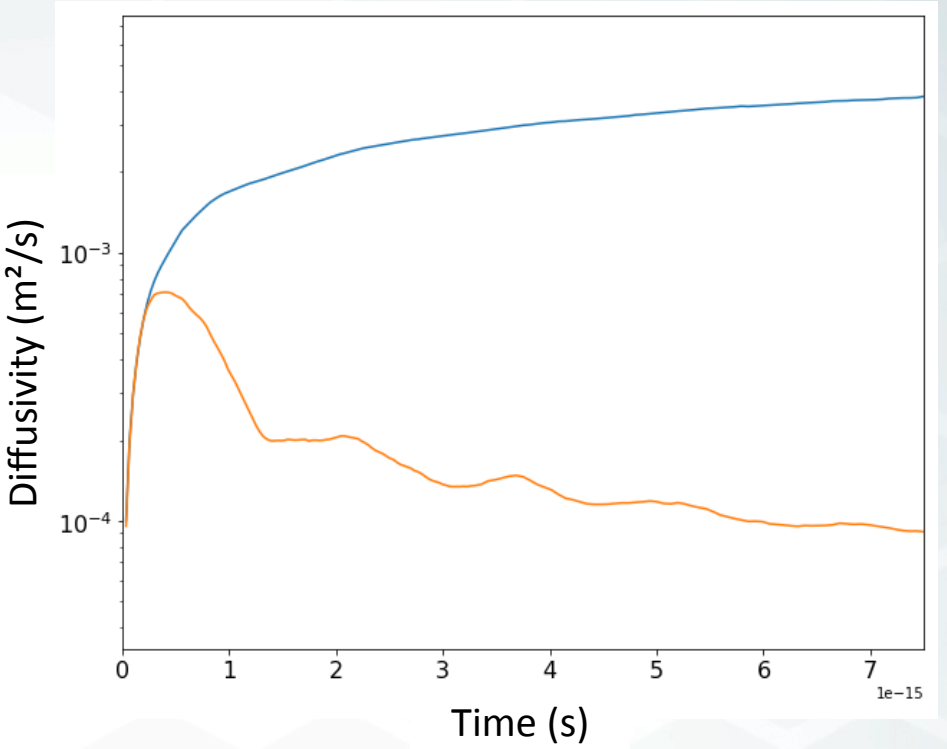

Electronic diffusivity as a function of time for a low disordered system (blue) and disordered system (orange)

Electronic transport and diffusion

- Temporal propagation of the wave function solved numerically
- Computation of the mean squared displacement : ΔX^2
- Electronic diffusivity :

$$D = \frac{\Delta X^2}{t}$$

- Electronic mobility observed experimentally : 5~50 cm²/V.s

$$\mu = \frac{eD}{2k_bT}$$

- Three different types of diffusion

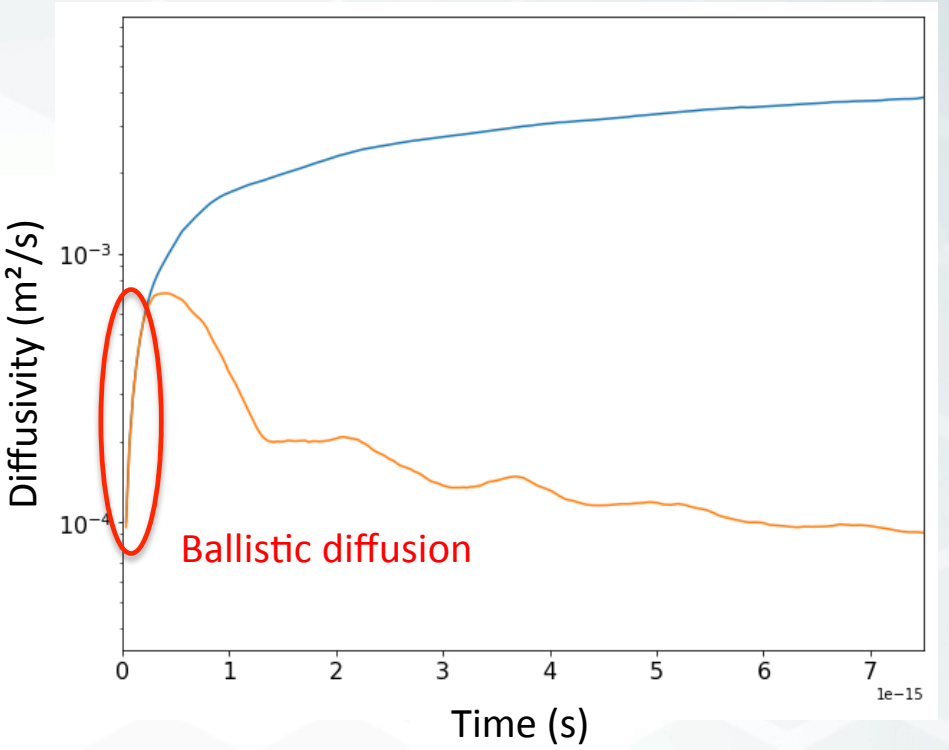

Electronic diffusivity as a function of time for a low disordered system (blue) and disordered system (orange)

Electronic transport and diffusion

- Temporal propagation of the wave function solved numerically
- Computation of the mean squared displacement : ΔX^2
- Electronic diffusivity :

$$D = \frac{\Delta X^2}{t}$$

- Electronic mobility observed experimentally : 5~50 cm²/V.s

$$\mu = \frac{eD}{2k_bT}$$

- Three different types of diffusion

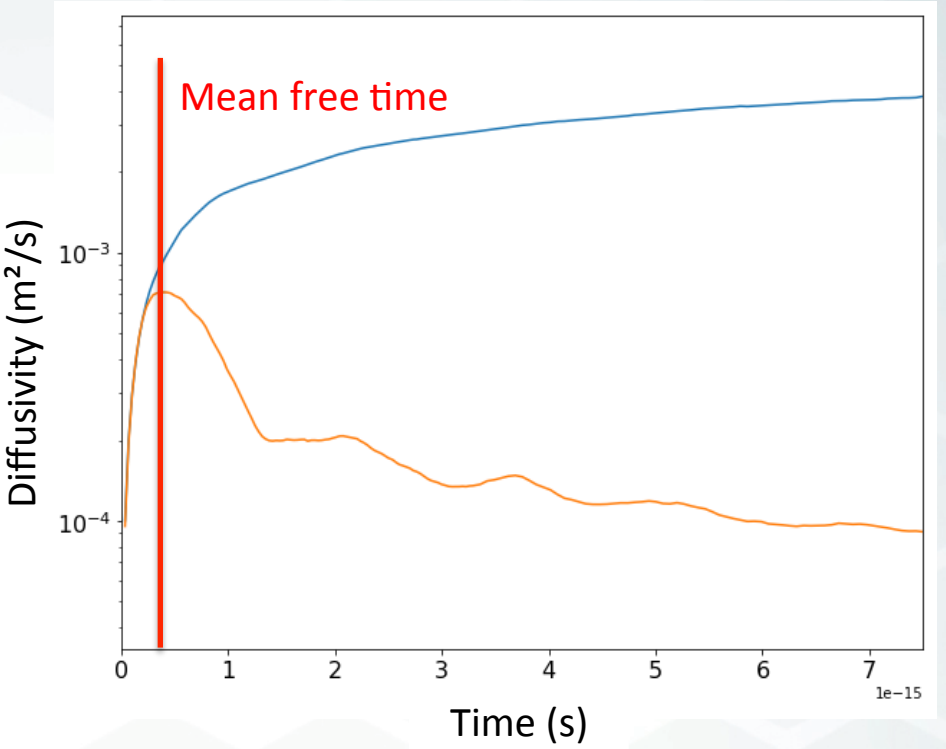

Electronic diffusivity as a function of time for a low disordered system (blue) and disordered system (orange)

Electronic transport and diffusion

- Temporal propagation of the wave function solved numerically
- Computation of the mean squared displacement : ΔX^2
- Electronic diffusivity :

$$D = \frac{\Delta X^2}{t}$$

- Electronic mobility observed experimentally : 5~50 cm²/V.s

$$\mu = \frac{eD}{2k_bT}$$

- Three different types of diffusion

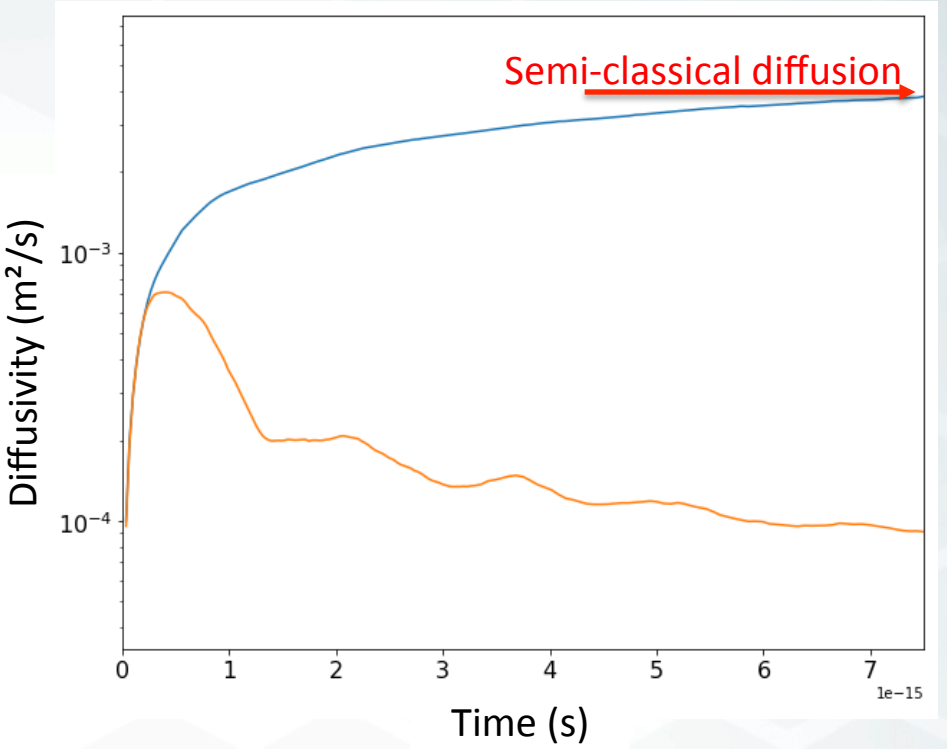

Electronic diffusivity as a function of time for a low disordered system (blue) and disordered system (orange)

Electronic transport and diffusion

- Temporal propagation of the wave function solved numerically
- Computation of the mean squared displacement : ΔX^2
- Electronic diffusivity :

$$D = \frac{\Delta X^2}{t}$$

- Electronic mobility observed experimentally : 5~50 cm²/V.s

$$\mu = \frac{eD}{2k_bT}$$

- Three different types of diffusion

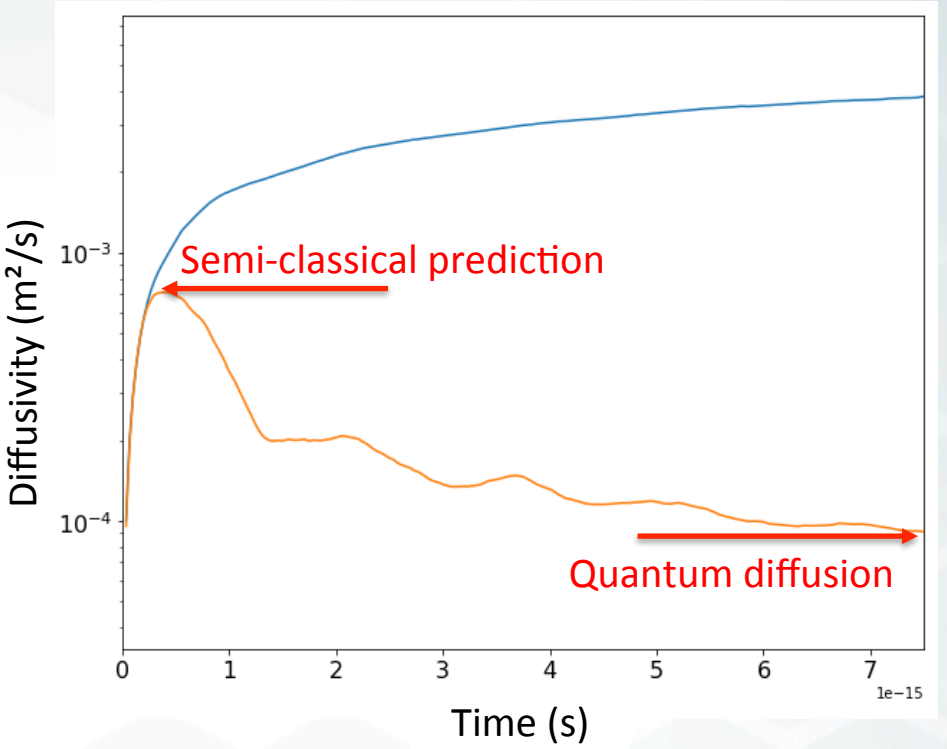

Electronic diffusivity as a function of time for a low disordered system (blue) and disordered system (orange)

Electronic transport and diffusion

- Mobility in good agreement with experimental results for both models
- Computed mean free path : ~0,5 nm
- Mean free path smaller than the primitive cell

  → Boltzmann's model requirements not respected
- Strong ratio classical μ/ computed μ at the top of the valence band
- Important localizations effect

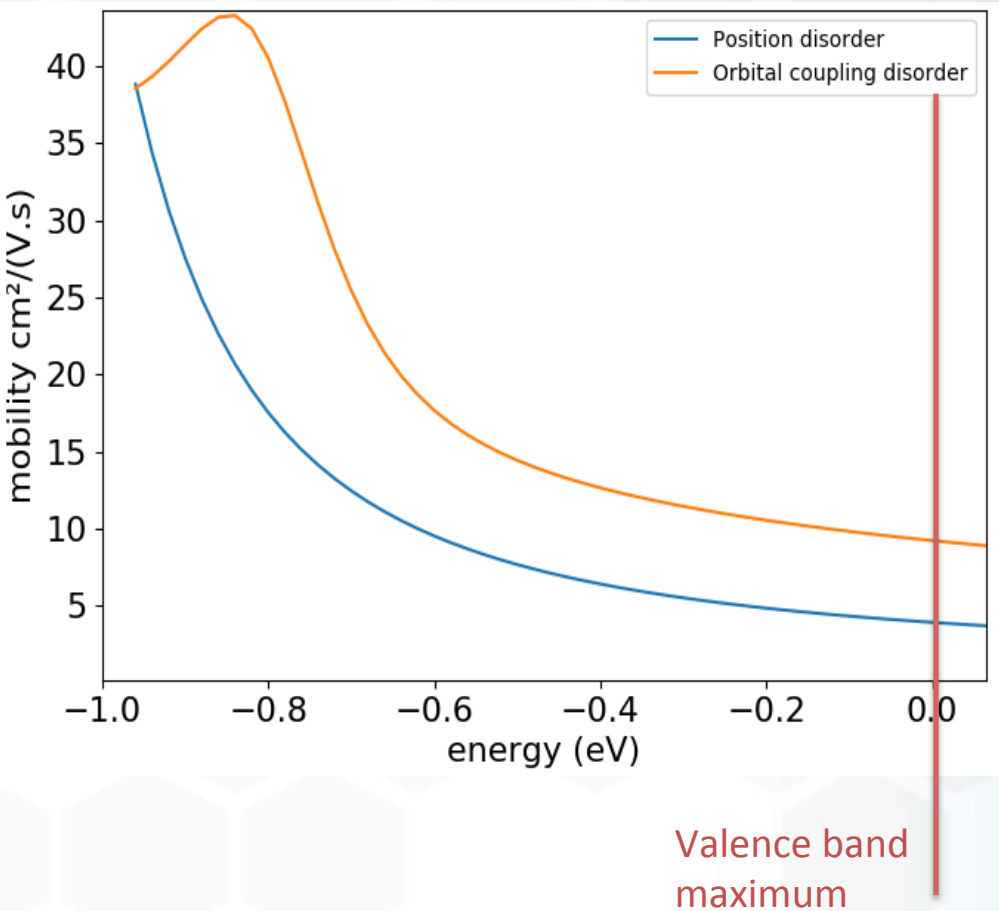

Electronic transport and diffusion

- Mobility in good agreement with experimental results for both models
- Computed mean free path : ~0,5 nm
- Mean free path smaller than the primitive cell

  → Boltzmann's model requirements not respected
- Strong ratio classical μ/ computed μ at the top of the valence band
- Important localizations effect

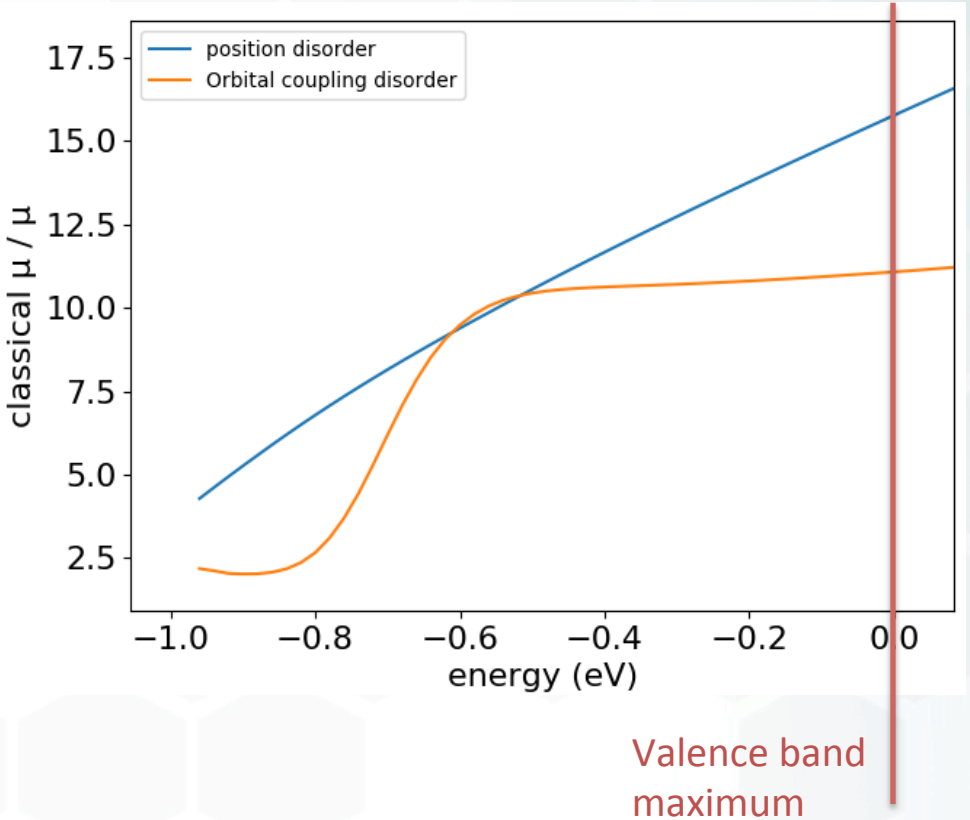

Physical principle of solar cells

19th December 2017

didier.mayou@neel.cnrs.fr

Optical Thz conductivity and quantum diffusion

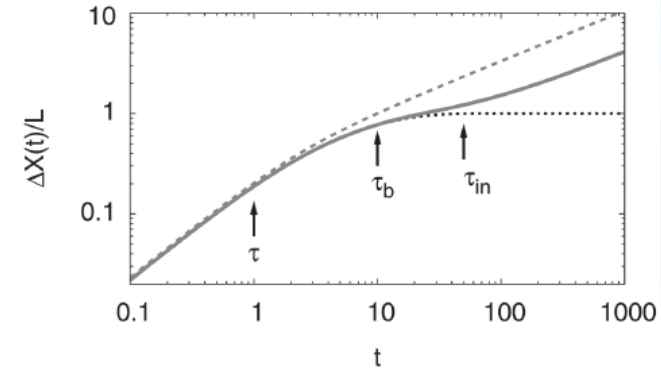

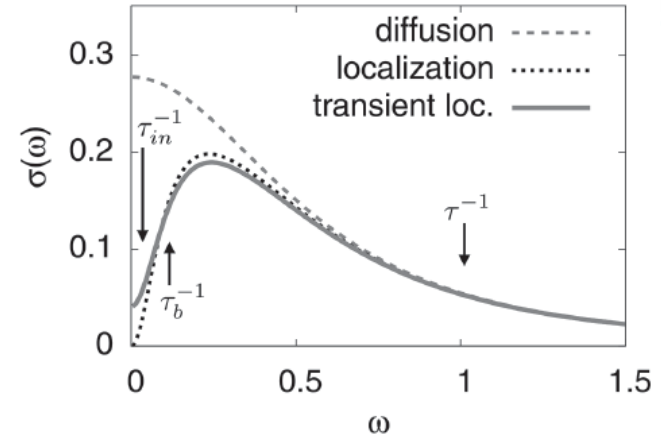

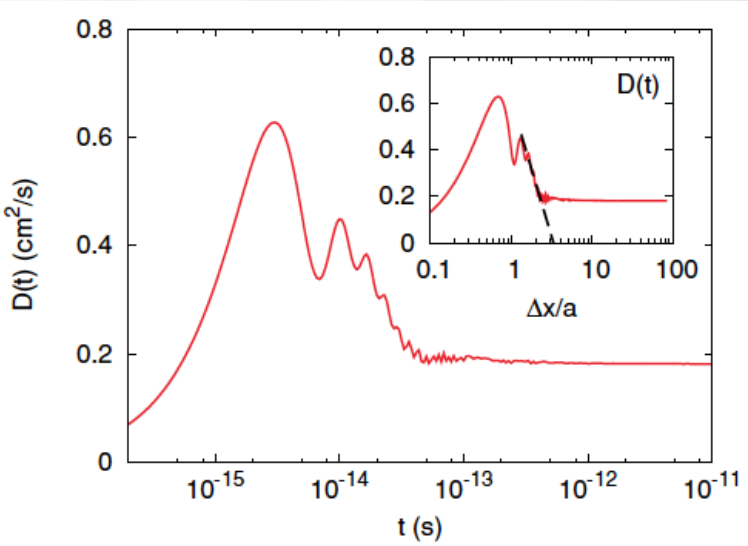

FIG. 2. (Color online) Time-dependent electron diffusivity $D(t)$ extracted via Eq. (4) from the experimental optical conductivity of Ref. 16 in the direction of highest conduction. The absolute value is fixed by the measured mobility $\mu \simeq 7\ \mathrm{cm}^2/Vs$. The inset shows the same quantity as a function of the instantaneous electron spread. The dashed line is the weak localization extrapolation.

$$\sigma(\omega) = -\frac{e^2\omega^2}{\nu}\frac{\tanh(\beta\hbar\omega/2)}{\hbar\omega}\mathrm{Re}\int_0^\infty e^{i\omega t}\Delta X^2(t)dt$$

$$\Delta x^2(t) = \frac{2\hbar}{\pi e^2}\mathrm{Re}\int_0^\infty (1-e^{-i\omega t})\frac{\sigma(\omega)/n}{\omega\tanh(\beta\hbar\omega/2)}d\omega$$

Optical conductivity

- Shape of the curves show clear signs of non classical-effects
- Both model consistent for the high energy limit
- Disorder based on position is the most coherent with the experimental results
- Maximum of conductivity:
  - ~8 meV

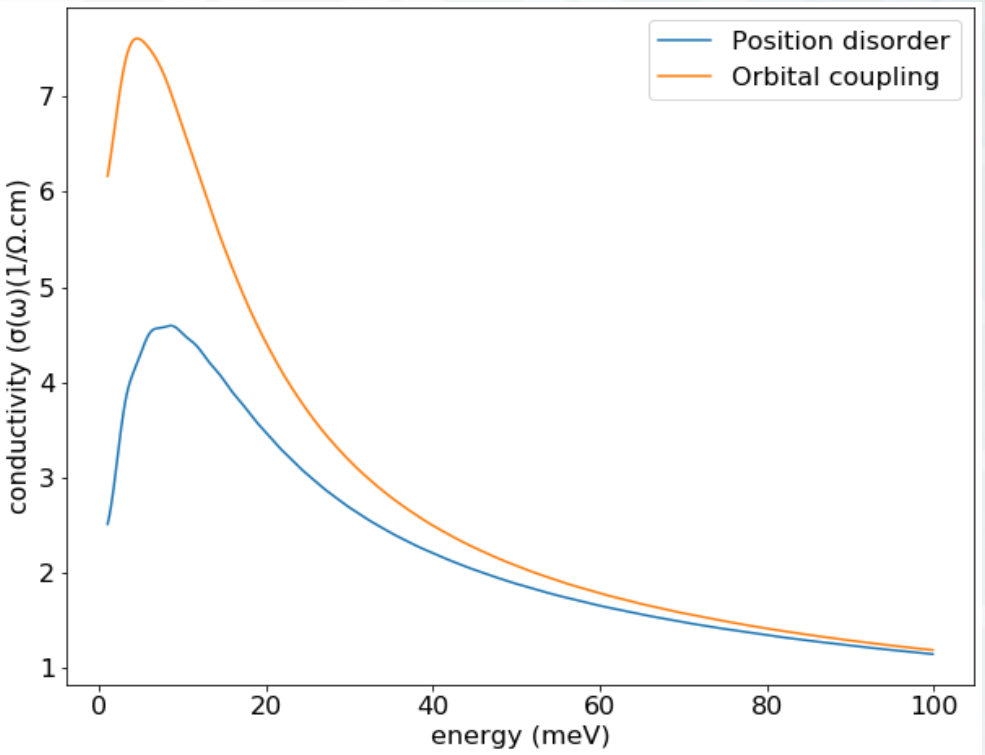

Optical conductivity

- Shape of the curves show clear signs of non classical-effects
- Both model consistent for the high energy limit
- Disorder based on position is the most coherent with the experimental results
- Maximum of conductivity:
  - ~8 meV

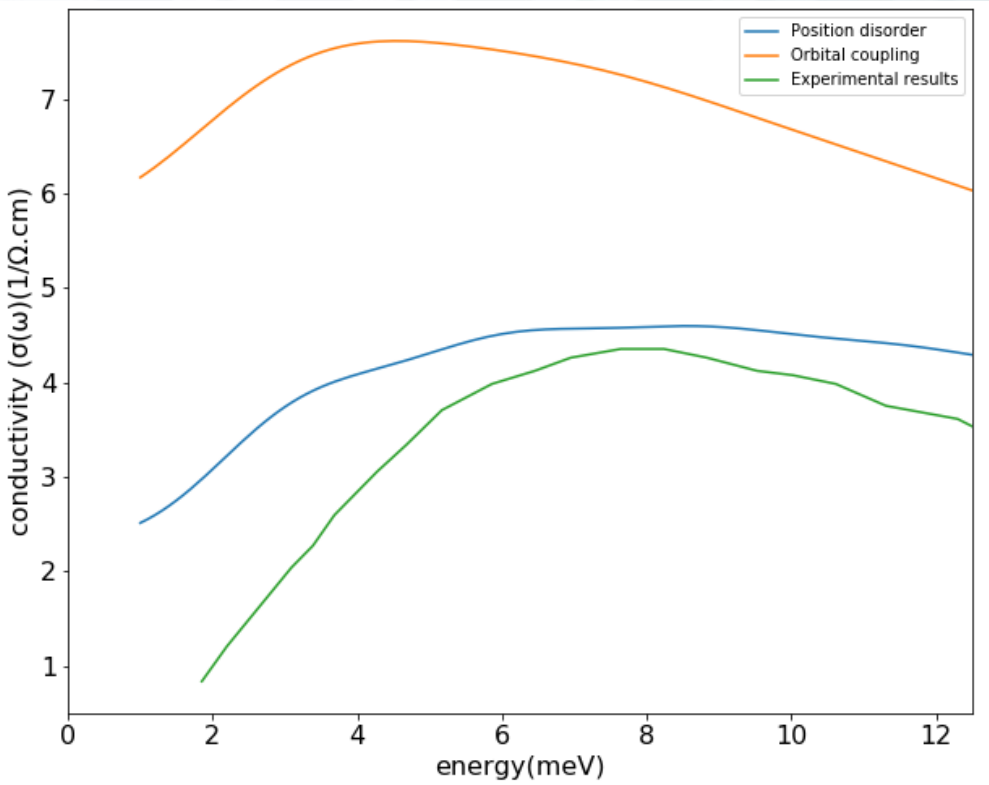

Message to take home

- Remarkable combination of properties of halide perovskite (small recombination of charges , relatively good mobilities, easy synthesis…)

- Complex systems which basic physics is not so well understood : why small recombination, charge transport, role of organic molecules…

CONCLUSIONS

- P-n planar junction: mature technology. In particular silicon dominates the market.
- Perovskites look like a very promising PV solution with application in other domains of opto-electronic
- Excitonic solar cells with organic semi-conductors or dye solar cells attract less attention but…who knows ?
- Photo-synthesis mechanisms attract much attention and are a source of inspiration : artificial photo-synthesis, solar fuels